Trajectory Tracking Control for a Boost Converter Based on the Differential Flatness Property

LEOPOLDO GIL-ANTONIO[1,2], BELEM SALDIVAR [1,3], OTNIEL PORTILLO-RODRÍGUEZ[1], GERARDO VÁZQUEZ-GUZMÁN[4], AND SAÚL MONTES DE OCA-ARMEAGA[5]

[1]Faculty of Engineering, Autonomous University of the State of Mexico, Toluca 50130, Mexico
[2]Tecnológico de Estudios Superiores de Jocotitlán, Jocotitlán 50700, Mexico
[3]Cátedras CONACYT, Ciudad de México 03940, Mexico
[4]Laboratory of Electricity and Power Electronics, Technological Institute of Superior Studies of Irapuato, Irapuato 36821, Mexico
[5]Bioengineering Department, Tecnológico de Monterrey, Toluca 50110, Mexico

Corresponding authors: Belem Saldivar (bsaldivarm@uaemex.mx) and Otniel Portillo-Rodríguez (oportillor@uaemex.mx)

ABSTRACT This paper presents the control design for the regulation and trajectory tracking tasks of the non-minimum phase output voltage of a DC-DC Boost-type power converter. The proposed approach exploits the differential flatness property of the system leading to a control strategy whose benefits include a simple derivation based on the parameterization of the control input and a zero steady-state error in the system response due to the establishment of predefined stable error dynamics. The main contribution of this paper is that the proposed controller is robust against power supply variations that may arise from the use of renewable energy sources. Furthermore, it is also robust against load variations that are normally related to energy consumption demands. These aspects are disregarded in most of the existing control techniques. Successful validation of the effectiveness of the flatness-based control system is carried out through numerical simulations and experimental tests performed in a built prototype of the system.

INDEX TERMS Control design, DC-DC power converters, differential flatness, nonlinear control systems, trajectory tracking task.

I. INTRODUCTION

In recent years, DC-DC power converters have been used in different applications such as switching power supplies, DC motor drives, photovoltaic systems, etc. [1]–[4]. The high efficiency in the input-output energy conversion of DC-DC power conversion systems is one of its salient features [5], [6]. The Boost-type converter is one of the basic topologies of DC-DC power converters which transforms a low input voltage into a high output voltage. Generally, its operation is controlled via the switching element through a Pulse-Width-Modulator (PWM) technique [7].

The difficulties in controlling Boost-type DC-DC converters lie in their nonlinear nature and in the existent input disturbances and parameter variations [8]. Unknown fluctuations of both the load and the input voltage degrade the performance of the controllers [9]. Input voltage variations are an often-encountered phenomenon that may arise from the use of non-conventional power supplies such as photovoltaic

energy [10], hydrogen fuel cells [11], or fading DC voltage sources [6], [12].

An effective control law for the trajectory tracking task must spontaneously respond even under system disturbances. Such performance is useful in dynamic applications such as motor drives or power converters to meet tracking requirements [13]. In the literature, there are different algorithms which have been proposed to control the output voltage of the Boost converter for the regulation and trajectory tracking tasks. For instance in [14], a control strategy that combines a predesigned cascade controller and a nested reduced-order Proportional-Integral Observers (PIOs) to produce a desired voltage is developed; the validity of the proposed observer-based control scheme is evaluated via computer simulations and comparative experiments using a laboratory prototype. A robust nonlinear adaptive controller for trajectory tracking maneuvers of the output voltage on a Boost converter with uncertain time-varying parameters is presented in [6]; this proposal is compared with an adaptive Linear Quadratic Regulator (LQR) optimal control based on feedback linearization showing its superiority. A sliding mode controller for the

The associate editor coordinating the review of this manuscript and approving it for publication was Fangfei Li.

regulation task is developed in [15]; the controller takes into account the variations of the load and voltage reference of the Boost converter. A control for the Boost converter that combines sliding modes with a generalized PIO is presented in [16]; the observer is used to estimate the perturbations occurring in the system in order to increase its robustness. The effectiveness of the proposed controller is evaluated through numerical simulations and experiments. Another control that considers the sliding mode technique is proposed in [17]; the salient feature of this control scheme is that the controlled system has a total sliding motion without a reaching phase as in the conventional sliding mode control. The design of a PWM-based adaptive sliding-mode control is presented in [18]; it operates in spite of unknown loads and unknown power source. The proposal is evaluated through numerical simulations and experimental tests; a comparison with a conventional sliding-mode controller and with a Propotional-Integral (PI) control shows its effectiveness. In [8], a robust time-delay control for the regulation of the output voltage of the Boost converter is proposed; it uses a delayed switching input to the converter, where the voltage and current output variables are replaced by unknown dynamics and disturbances. The proposed control is validated through numerical simulations and experimental tests; its robustness is evaluated by means of load and input voltage variations.

A cascade control that embeds a robust inner-loop current controller for the task of regulating the output voltage of a Boost converter is developed in [19]; the performed experiments show the robustness of the proposed approach against uncertainties in both the system parameters and the converter load. A different controller for the stabilization task is presented in [20], it is based on the system passivity property in combination with two nonlinear observers that reject perturbations of the system parameters; a comparative analysis demonstrates the superiority of the proposed approach with respect to the classic passivity control and with respect to a passivity control with integral action. The cascade controller proposed in [21] is based on a reduced order PIO for regulating the voltage of the Boost converter that is subject to various uncertainties such as changes in load resistance, power supply variations and parametric uncertainties. This control is validated through numerical simulations.

The above-mentioned references deal with the regulation task. On the other hand, the trajectory tracking problem for the Boost converter is addressed in [22] and [23]. In [22], a flat filter digital controller based on the flatness property is designed and implemented. The flat filter constitutes a reinterpretation of the classical compensation networks for linear systems. In [23], a sliding mode controller in which the reference signal is defined by the flat output of the system is designed and validated by means of experimental tests. Nevertheless, the chattering phenomenon linked to the sliding mode technique and the lack of robustness against load variations are some of its drawbacks.
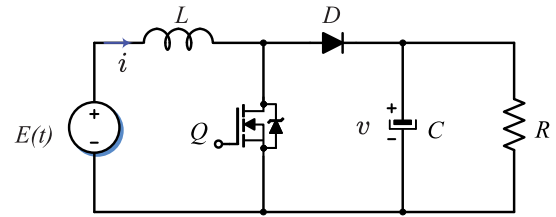

FIGURE 1. Electronic circuit of a Boost converter.

The differential flatness property of the Boost converter has been used to obtain the parameterization of the system variables, see for instance [24]. Within the framework of the trajectory tracking problem, this parameterization is useful for generating the reference trajectories in terms of intrinsic variables of the system, see for instance [23]–[27]. Based on this approach a trajectory tracking feedback controller with integral action is derived in [24].

Following the ideas presented in [24] and motivated by the parametrization technique used in [23]–[27], this paper details the design of a closed-loop controller oriented to the regulation and trajectory tracking tasks for the output voltage of the Boost converter. It is important to highlight that the proposed control approach operates under power supply variations typically arising from the use of renewable energy sources. In contrast, this aspect is disregarded in most of the existing control techniques. Besides, unlike other research works, the proposed control is robust against load variations that are normally related to energy consumption demands. The effectiveness of the flatness-based controller is validated through numerical simulations and experimental tests performed in a built prototype of the system. Among the advantages of the proposed controller, it is worth mentioning that its derivation and implementation are simple. Besides, there is no steady state error in the system response due to the establishment of predefined stable error dynamics.

It is worth mentioning that the output voltage of the Boost converter is of non-minimum phase, which hinders the control design since the related dynamic is unstable around the equilibrium point [28], [29]. However, it has been shown that the flatness approach allows controlling non-minimal phase systems [24], [30].

The rest of the paper is organized as follows. Section II presents a general description and the mathematical model of the DC-DC Boost converter. Section III details the design of a differential flatness-based controller. Section IV highlights the effectiveness of the proposed controller through simulation and experimental results. Finally, section V presents some concluding remarks and perspectives.

II. DC-DC BOOST CONVERTER MODEL
The main attribute of the Boost converter is that its output voltage is always equal to or greater than its input voltage. Fig. 1 shows the electronic diagram of a Boost power converter consisting of the following elements: an inductor L, a capacitor filter C, a load resistor R, a diode D, and a
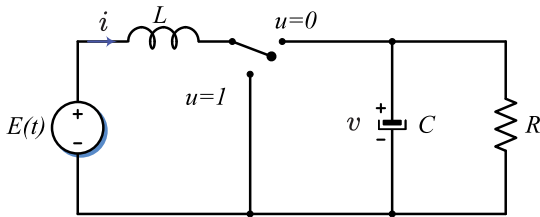
FIGURE 2. Ideal circuit of a Boost converter.

transistor Q, which operates within the cut-off and saturation regions when it is excited by a switched signal. In order to represent the ideal model of the Boost converter, it must be considered that the transistor has an infinitely fast response and that the diode has a threshold voltage equal to zero, which allows the activation of conducting and blocking states without any time loss. Here it is assumed that the input voltage $E(t)$ is provided by a variable power source.

Fig. 2 shows the electronic diagram of an ideal Boost power converter. Note that the transistor and the diode are replaced here by a switching device with two positions indicated as $u = 1$ and $u = 0$. When $u = 1$, there is no connection between the voltage source $E(t)$ and the system load R, and when $u = 0$, the energy flows between the power supply and the load. The Boost converter output voltage is then controlled by the switch position u. Generally, the switch position change is carried out by a PWM signal.

Kirchhoff's voltage and current laws are used to obtain the mathematical model of the Boost converter described by the differential system given by [1]:

$$\frac{di}{dt} = -\frac{v}{L}(1 - u) + \frac{E}{L} \qquad (1)$$

$$\frac{dv}{dt} = \frac{i}{C}(1 - u) - \frac{v}{RC} \qquad (2)$$

where v is the output voltage, i is the current through the inductor, and E is the time-varying power supply voltage. The control input u represents the switch position which can only take the binary values $\{0,1\}$.

A. AVERAGE MODEL

In order to design a control law for the Boost converter an average model must be defined. The average model of the Boost converter is represented by the same equations (1)-(2), but the control variable u is redefined as a sufficiently smooth function u_{av} taking values in the real interval [0,1] representing the average switch position and i, v are the average variables of the system. Then, the model given by (3)-(4) is referred to as average model replacing the switched control input $u \in \{0, 1\}$ by the average control input $u_{av} \in [0, 1]$, which is frequently interpreted as a duty ratio function in PWM-controlled converters and as the equivalent control in sliding mode-controlled converters [24].

[1] In the following, the time dependence symbol (t) of dynamic variables will be omitted for simplification.

The average model is written as:

$$\frac{di}{dt} = -\frac{v}{L}(1 - u_{av}) + \frac{E}{L} \qquad (3)$$

$$\frac{dv}{dt} = \frac{i}{C}(1 - u_{av}) - \frac{v}{RC} \qquad (4)$$

where the capacitor voltage v is a non-minimum phase output, while the inductor current i is a minimum phase output.

Regarding the mathematical model of the Boost converter used in this paper, it should be mentioned that despite being a model where energy losses are not considered, it is used due to its simplicity and relatively good precision compared to more complex models such as the ones that consider the internal resistance of the inductor, the Shockley diode model [31], or the Ebers-Moll transistor model [32].

III. FLATNESS-BASED CONTROL DESIGN

In nonlinear systems theory, the flatness property refers to the capability of dynamic systems to support an accurate linearization through endogenous feedback [33]. A differentially flat system is one that satisfies the flatness property. The main feature of differentially flat systems is that the input and state variables can be defined in terms of a set of variables, known as flat output or linearizing output, and a finite number of its time derivatives without integrating the underlying differential equation.

A flat output of the Boost converter can be determined by the total energy stored in the system (see for instance [23]– [27], [34]):

$$F = \frac{1}{2}\left(Li^2 + Cv^2\right) \qquad (5)$$

Using (3) and (4), the differential parameterization of the states and of the input of the Boost converter is obtained as follows:

$$i = -\frac{RCE}{2L} + \beta \qquad (6)$$

$$v = \sqrt{\frac{2}{C}F - \frac{L}{C}\left(-\frac{RCE}{2L} + \beta\right)} \qquad (7)$$

$$u_{av} = 1 - \frac{i\dot{E} + \frac{1}{L}E^2 + \frac{2}{R^2C}v^2 - \ddot{F}}{\left(\frac{1}{L}E + \frac{2}{RC}i\right)v} \qquad (8)$$

$$\beta = \frac{1}{2}\sqrt{\left(\frac{RCE}{L}\right)^2 + \frac{4}{L}\left(RC\dot{F} + 2F\right)} \qquad (9)$$

The derivation of (6)-(9) is presented in Appendix A. Note that the average model (3)-(4) is represented by the differential parameterization given by (6)-(9) stated in terms of the flat output F and its time derivatives.

The control objective is to steer the output voltage v to a predefined (constant or variable) reference v^*. To accomplish this goal, the control must force the flat output F to follow the predefined reference F^* calculated as:

$$F^* = \frac{1}{2}\left(Li^2 + Cv^{*2}\right) \qquad (10)$$

Note that F^* is given in terms of the predefined reference voltage v^* and of the corresponding inductor current i which, in practice, can be directly measured by a SP22 sensor, as will be seen in Section IV.

Following [24], in (8), the highest order derivative of the flat output is replaced by an auxiliary input (μ_{aux}), i.e.,

$$\mu_{aux} = \ddot{F} \tag{11}$$

Then, the control u_{av} is determined by:

$$u_{av} = 1 - \frac{i\dot{E} + \frac{1}{L}E^2 + \frac{2}{R^2 C}v^2 - \mu_{aux}}{\left(\frac{1}{L}E + \frac{2}{RC}i\right)v} \tag{12}$$

By an appropriate selection of the auxiliary input, the stable error dynamics ensure that $F \rightarrow F^*$, which means that the trajectory tracking task is achieved. The auxiliary input defined in (13) is considered.

$$\mu_{aux} = \ddot{F}^* - \beta_2(\dot{F} - \dot{F}^*) - \beta_1(F - F^*) - \beta_0 \int_o^t (F - F^*)d\tau \tag{13}$$

Define the error e as the difference between the actual flat output F and the one defined in terms of the reference output voltage F^*, i.e., $e = F - F^*$.

The closed-loop tracking error dynamics is obtained by substituting (13) in (11) and taking the time derivative of the resulting equation:

$$\dddot{e} + \beta_2\ddot{e} + \beta_1\dot{e} + \beta_0 e = 0 \tag{14}$$

The error will asymptotically converge to zero if the gains of the feedback tracking controller are chosen such that all roots of the characteristic polynomial of the closed loop system $p(s)$ defined in (15) lie in the left half complex plane. The constants β_2, β_1 and β_0 must be chosen accordingly.

$$p(s) = s^3 + \beta_2 s^2 + \beta_1 s + \beta_0 \tag{15}$$

The characteristic polynomial is written in terms of the damping factor ζ and the natural frequency ω_n as follows:

$$p(s) = (s + a)(s^2 + 2\zeta\omega_n s + \omega_n^2) \tag{16}$$

where $a > 0$, $\omega_n > 0$ and $\zeta > 0$. Notice that β_2, β_1 and β_0 are determined by:

$$\beta_2 = 2\zeta\omega_n + a, \quad \beta_1 = 2a\zeta\omega_n + \omega_n^2, \quad \beta_0 = a\omega_n^2 \tag{17}$$

Notice also that the proposed control law defined in (12)-(13) takes into account that the input voltage E is a time-varying function. However, load resistance variations are not considered in the control design. The presence of such variations can be monitored in real-time through the measurement of the current flowing through this element i_R. Then, in this way the control is robust against load and input voltage variations. The closed loop system trajectories are free of steady state error due to the predefined stable dynamic. The average controller defined in (12)-(13) cannot appropriately govern the DC-DC Boost converter switch since it only takes binary
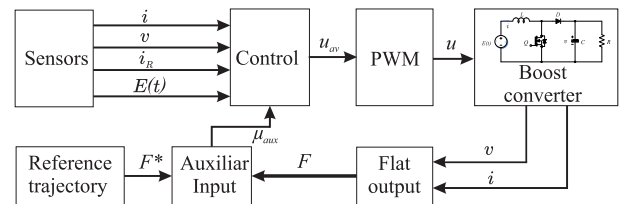

FIGURE 3. Block diagram of the flatness-based control system.
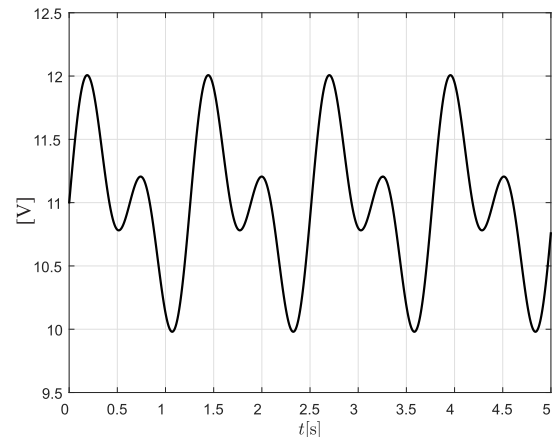

FIGURE 4. Time-varying input voltage, $E(t)$.

values, hence, the controller can be implemented through a PWM [35]. Figure 3 presents a schematic diagram illustrating the implementation of the control system. Notice that the reference flat output F^* is generated from the reference voltage v^* through (10).

IV. NUMERICAL SIMULATIONS AND EXPERIMENTAL IMPLEMENTATION

This section presents the numerical simulations and the experimental tests performed in a built prototype of the system for the validation of the flatness-based controller developed in the previous section.

A. NUMERICAL SIMULATIONS
The performance of the proposed control approach is evaluated through numerical simulations using the software Matlab®/Simulink®. The following model parameters were considered.

$$L = 10\text{mH}, \ C = 470 \ \mu\text{F}, \ R = 50 \ \Omega$$

Fig. 4 shows the time-varying input voltage $E(t)$ defined by

$$E(t) = 11.008 + 0.5504\sin(5t) + 0.5848\sin(10t),$$
$$10 \ V \le E(t) \le 12 \ V$$

The design parameters defined in (17) are chosen as $\beta_0 = 12500000$, $\beta_1 = 280000$, and $\beta_2 = 650$, so that

$$a = 50, \quad \zeta = 0.6, \ \omega_n = 500. \tag{18}$$

Then, the roots of the characteristic polynomial (15) are $s_1 = -100 + 4j$, $s_2 = -100 - 4j$ and $s_3 = -50 + 0j$.
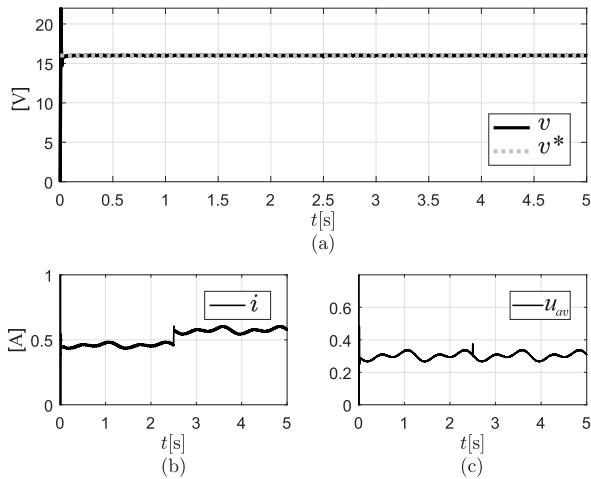
FIGURE 5. Numerical simulations for the first study case: constant reference signal, variation in the load resistance. (a) Boost converter output voltage; (b) inductor current response; (c) flatness-based average control signal.
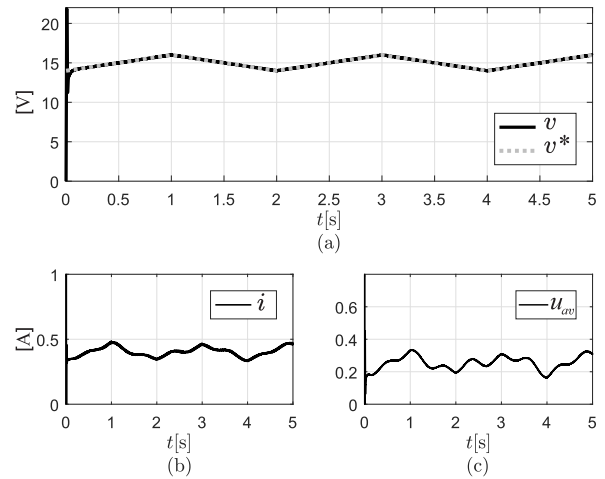

FIGURE 6. Numerical simulations for the second study case: triangular reference signal. (a) Boost converter output voltage; (b) inductor current response; (c) flatness-based average control signal.

Since the roots lie on the left side of the complex plane, the stability of the error dynamics is ensured, i.e., the error $e = F - F^*$ asymptotically converges to zero as $t \to \infty$.

The performance of the flatness-based controller is evaluated through simulations. The following four study cases were considered.

(i) The converter output voltage must keep a constant value of 16 V. A variation in the load resistance at 2.5 seconds is considered. This variation is performed by connecting in parallel a resistance (R_p) of 220 Ω to the one of 50 Ω, which leads to an equivalent load of 40.7407 Ω. This variation demands to the Boost converter to handle an increment of 22.73% in the current. Simulation results for this study case are shown in Fig. 5.

(ii) The output voltage of the Boost converter must follow a triangular signal varying between 14 V and 16 V. The simulation results are shown in Fig. 6.

(iii) The output voltage of the Boost converter must follow a sine signal that varies between 14 V and 16 V with a period of 2.5 s. The simulation results are shown in Fig. 7.

(iv) The output voltage of the Boost converter must smoothly shift from an initial value of $v_i^* = 14$ V to a final value of $v_f^* = 16$ V in a time interval of 1 s. Subsequently, it must smoothly decrease from 16 V to 14 V. For this case, the reference trajectory $F^*(t)$ is defined as follows:

$$F^*(t) = \begin{cases} F^*(t_i), & \text{for } t < t_i \\ F^*(t_i) + (F^*(t_f) - F^*(t_i))f(t, t_i, t_f) \\ \quad \text{for } t_i \le t \le t_f \\ F^*(t_f), & \text{for } t > t_f \end{cases}$$
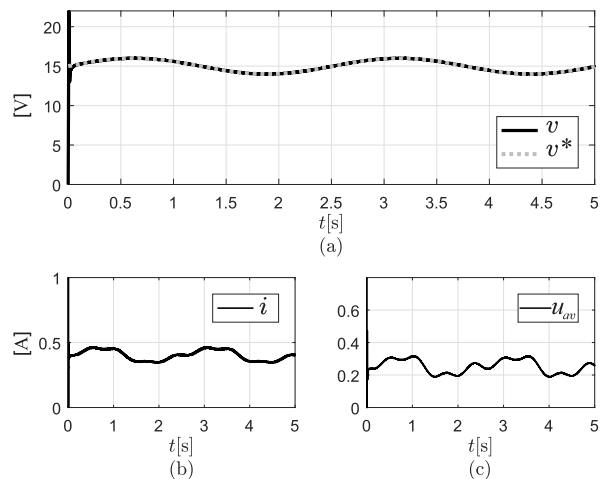

FIGURE 7. Numerical simulations for the third study case: sinusoidal reference signal. (a) Boost converter output voltage; (b) inductor current response; (c) flatness-based average control signal.

where $f(t, t_i, t_f) \in [0,1] \, \forall \, t \in [t_i, t_f]$ is a 10th-order Bézier polynomial defined as:

$$f(t, t_i, t_f) = 252\varphi^5 - 1050\varphi^6 + 1800\varphi^7 \\ - 1575\varphi^8 + 700\varphi^9 - 126\varphi^{10}$$

where

$$\varphi = \left(\frac{t - t_i}{t_f - t_i} \right)$$

and

$$F^*(t_i) = \frac{1}{2} \left(\frac{L v_i^{*4}}{R^2 E^2} + C v_i^{*2} \right)$$

$$F^*(t_f) = \frac{1}{2} \left(\frac{L v_f^{*4}}{R^2 E^2} + C v_f^{*2} \right)$$
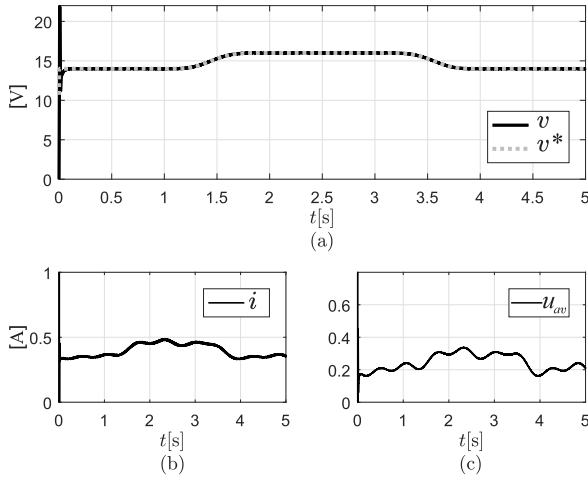
FIGURE 8. Numerical simulations for the fourth study case: smooth reference signal. (a) Boost converter output voltage; (b) inductor current response; (c) flatness-based average control signal.

FIGURE 9. Zoom of Figure 5 (a).

The initial values of the current and voltage of the Boost converter are:

$$\left[i^*(t_i), v^*(t_i)\right] = \left[\frac{v_i^{*2}}{RE}, v_i^*\right] = \left[\frac{14^2}{RE} \text{ A, } 14 \text{ V}\right]$$

and the final values are:

$$\left[i^*(t_f), v^*(t_f)\right] = \left[\frac{v_f^{*2}}{RE}, v_f^*\right] = \left[\frac{16^2}{RE} \text{ A, } 16 \text{ V}\right]$$

Fig. 8 shows the simulation results for the fourth study case.

The reference trajectories defined for v^* in cases (i)-(iv) are directly generated from Matlab$^{\circledR}$/Simulink$^{\circledR}$. According to the control system diagram shown in Figure 3, this signal v^* is sent to a block that, from (10), generates the reference flat output F^* which is required to produce the control signal.

Simulation results highlight the performance of the proposed control approach which is effective in solving the regulation and trajectory tracking tasks raised in the different test scenarios. Case (i) considers the transit from a lightly loaded system to a heavily loaded one; cases (ii)-(iv) are defined to demonstrate the effectiveness of the control law in tracking different reference trajectories. From Figures 5-8, it can be noticed that the system reaches the steady state in a very short period of time regardless the variation of the power supply voltage. Besides, the load change occurring at 2.5 s is imperceptible in the output voltage response. A zoom of Figure 5 (a) shows that the stabilization time is acceptable since it is less than 0.05 s (see Figure 9). As can be seen, a time-varying power supply voltage does not prevent the control from solving the regulation and trajectory tracking tasks and a change in the load do not degrade the performance of the flatness-based controller.

B. EXPERIMENTAL RESULTS

This section presents the experimental results that highlight the effectiveness of the proposed control strategy.
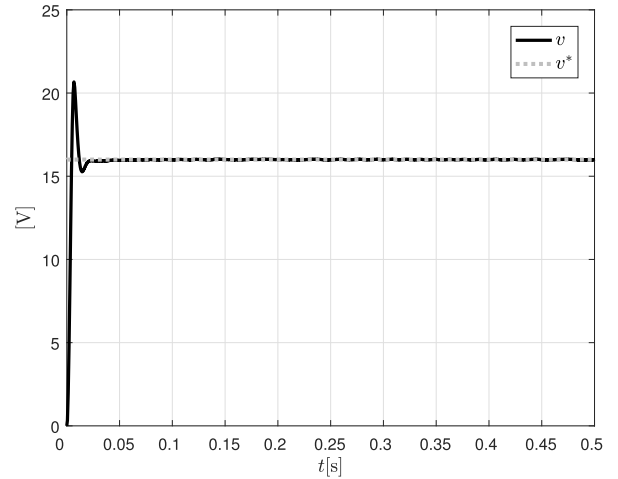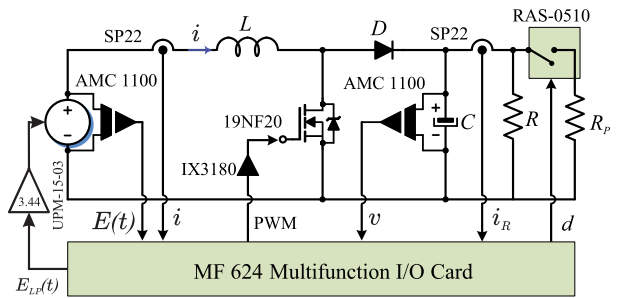

FIGURE 10. General scheme of a experimental setup of the Boost converter.

For the implementation of the flatness-based controller, a Boost power converter is designed to operate in continuous conduction mode (CCM) at a switching frequency of 45 KHz. Furthermore, four sensors are used to measure the following variables: the current through the inductor i, the output voltage of the converter v, the input voltage E and the current through the load resistor i_R. An additional circuit enables the change in the system load by means of a digital output signal d.

Fig. 10 shows a diagram with the Boost converter elements and their part numbers. The flatness-based control algorithm was implemented with the Simulink Real-Time$^{\circledR}$ software using an Humusoft$^{\circledR}$ MF 624 multifunction I/O card that is installed on a computer with an Intel$^{\circledR}$ $Core^{TM}$ i7 processor and 8GB RAM memory. The complete scheme operates at a fixed sampling frequency of 10 KHz. A PWM generator which is set to a frequency of 45 KHz, four analog inputs to sense the current and voltage, one analog output to generate the low power source signal $E_{LP}(t)$ and a digital output allowing the load change were implemented. The disturbance signal d uses a digital output of the MF 624 card, which has a voltage level of 5 V when $d = 1$; its function is to activate the relay RAS-0510. Since the Humusoft$^{\circledR}$ card can only generate analog signals with maximum values of $\pm$ 10 Volts with a maximum current of
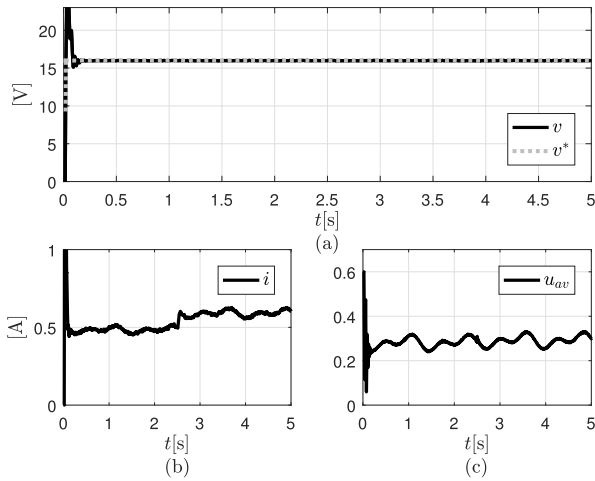
FIGURE 11. Experimental results for the first study case: constant reference signal, variation in the load resistance. (a) Boost converter output voltage; (b) inductor current response; (c) flatness-based average control signal.
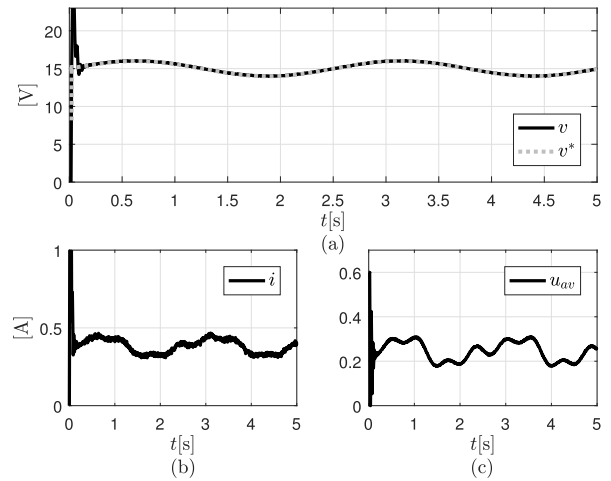

FIGURE 12. Experimental results for the second study case: triangular reference signal. (a) Boost converter output voltage; (b) inductor current response; (c) flatness-based average control signal.

FIGURE 13. Experimental results for the third study case: sinusoidal reference signal. (a) Output voltage response; (b) inductor current; (c) average control input.
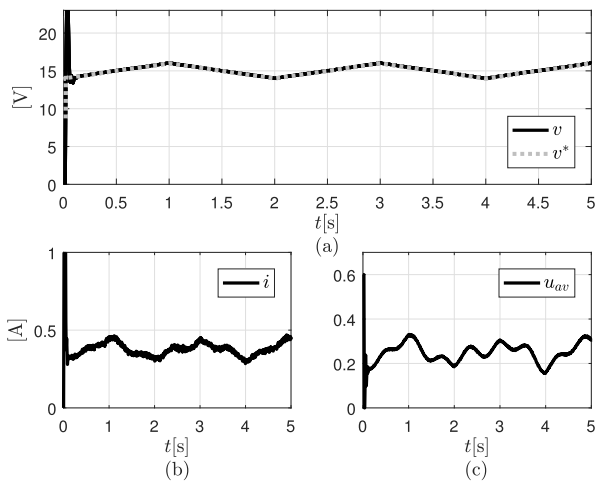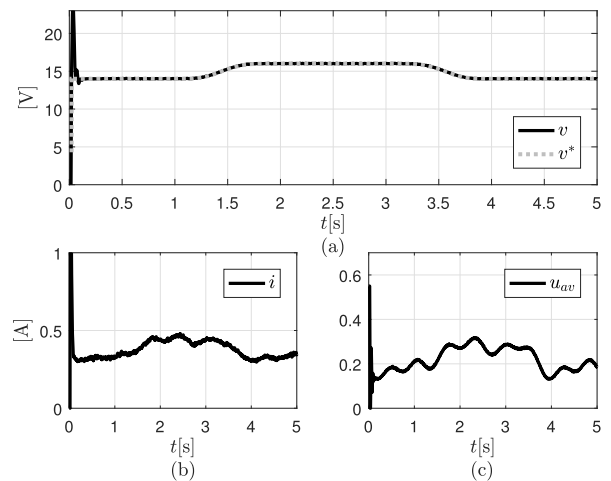

FIGURE 14. Experimental results for the fourth study case: smooth reference signal. (a) Output voltage response; (b) inductor current; (c) average control input.

$\pm$ 15 mA, to generate the signal $E(t)$ it was necessary to amplify by a factor of 3.44 the signal $E_{LP}(t) = 3.2 + 0.16 \sin(5t) + 0.17 \sin(10t)$ by means of a linear operational amplifier based on the Quanser® card UPM-15-03 (with maximum values of: $\pm$ 15 Volts, $\pm$ 3 A, 45 Watts continuous) in non-inverter mode.

The flatness-based control system can be described as follows (use Figures 3 and 10 as visual guides). The input signals to the average control defined in (12) are supplied by sensors S22P (current) and AMC1100 (voltage). The average control signal u_{av} adjusts the duty cycle of the PWM generator operating at a frequency of 45 KHz, which activates the MOSFET 19NF20 through the optocoupler circuit IX3180. The auxiliary input μ_{aux} defined in (13) is generated with the use of the reference signal F^* (derived from the output voltage reference) and the flat output F.

The four study cases described in the previous section were also considered for the development of experimental tests.

Fig. 11 shows the experimental results obtained for the first study case in which the output voltage of the Boost converter must follow a constant reference signal and a variation in the load resistance at 2.5 seconds is considered.

Fig. 12 shows the results for the second study case in which the output voltage of the Boost converter must follow a triangular reference signal.

Similarly, Fig. 13 shows the experimental results obtained for the third study case in which the output voltage of the Boost converter must follow a sinusoidal reference signal.

Fig. 14 shows the experimental results obtained for the fourth study case in which the output voltage of the Boost converter must follow a reference signal that smoothly increases from 14 V to 16 V and then smoothly decreases from 16 V to 14 V.

It is worth mentioning that, despite the chattering, the proposed control approach is robust against load and voltage
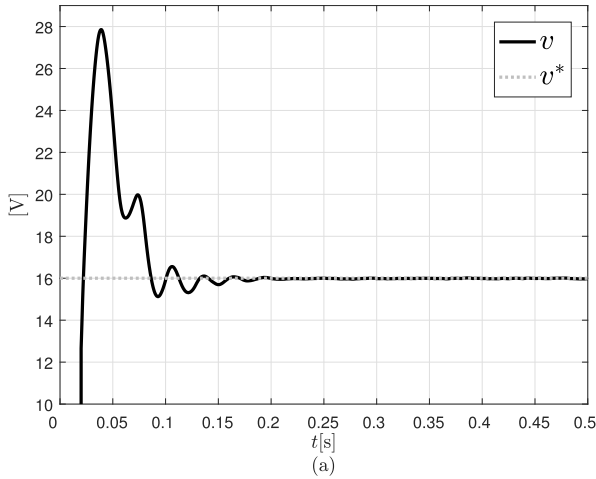
FIGURE 15. Zoom of Figure 11 (a).

supply variations. For a better perception of the system response characteristics, a zoom of Figure 11 (a) is presented in Figure 15. Due to the control action, the system response presents an overshoot, which is of greater magnitude compared to the one obtained in the simulation (see Figure 9). The settling time is also bigger, but still it can be considered acceptable since it is less than 0.2 s and most applications do not require a faster response.

V. CONCLUSION AND PERSPECTIVES

The design of an average control based on the differential flatness property of a DC-DC Boost power converter in which the output voltage requires to steer a desired reference voltage is presented in this paper. The proposed control scheme is shown to be robust against power supply and load variations. In practice, the power supply variations are associated with renewable energy sources which do not always deliver a constant voltage and the load variations are related to energy consumption demands. An efficient performance of the proposed control scheme was observed both in numerical simulations and in experimental results. Among the benefits of the controller are its direct derivation from the differential parameterization of the control input and its simple implementation. Furthermore, the trajectories are driven to the reference paths without steady state error and with a short settling time.

In order to illustrate the robustness of the proposed approach against power supply variations in a practical application, authors are working on the experimental implementation of the flatness-based controller to solve the Maximum Power Point Tracking (MPPT) problem in a photovoltaic system. The MPPT problem can be treated as a trajectory tracking problem for which the reference trajectory is described in terms of the maximum power provided by the photovoltaic panel.

APPENDIX A DIFFERENTIAL PARAMETERIZATION

This section presents the parameterization of the states and control inputs of the Boost converter model derived from the

flat output. Consider the flat output given by

$$F = \frac{1}{2}\left(Li^2 + Cv^2\right) \qquad (19)$$

Its time derivative is:

$$\dot{F} = Li\frac{di}{dt} + Cv\frac{dv}{dt} \qquad (20)$$

substituting the system dynamics (3)-(4) yields,

$$\dot{F} = i(-vu + E) + v(iu - \frac{v}{R})$$

$$\dot{F} = iE - \frac{v^2}{R} \qquad (21)$$

where

$$u = 1 - u_{av} \qquad (22)$$

The parameterization of i is obtained by substituting v^2 (that can be derived from (21)) into 19,

$$i = -\frac{RCE}{2L} + \beta \qquad (23)$$

where:

$$\beta = \frac{1}{2}\sqrt{\left(\frac{RCE}{L}\right)^2 + \frac{4}{L}\left(RC\dot{F} + 2F\right)} \qquad (24)$$

From (19), one obtains:

$$v = \sqrt{\frac{2F - Li^2}{C}} \qquad (25)$$

substituting (23) into (25) yields the parameterization of v, which is obtained as follows:

$$v = \sqrt{\frac{2}{C}F - \frac{L}{C}\left(-\frac{RCE}{2L} + \beta\right)^2} \qquad (26)$$

The second derivative of F is:

$$\ddot{F} = i\dot{E} + E\frac{di}{dt} - \frac{2v}{R}\frac{dv}{dt} \qquad (27)$$

Substituting the system dynamics (3)-(4) into (27) yields the parameterization of the average control as follows:

$$u_{av} = 1 - \frac{i\dot{E} + \frac{1}{L}E^2 + \frac{2}{R^2C}v^2 - \ddot{F}}{\left(\frac{1}{L}E + \frac{2}{RC}i\right)v} \qquad (28)$$

REFERENCES

[1] H. Sira-Ramírez, R. A. Pérez-Moreno, R. Ortega, and M. García-Esteban, "Passivity-based controllers for the stabilization of DC-to-DC power converters," *Automatica*, vol. 33, no. 4, pp. 499–513, Apr. 1997.

[2] R. Silva-Ortigoza, V. M. Hernández-Guzmán, M. Antonio-Cruz, and D. Muñoz-Carrillo, "DC/DC buck power converter as a smooth starter for a DC motor based on a hierarchical control," *IEEE Trans. Power Electron.*, vol. 30, no. 2, pp. 1076–1084, Feb. 2015.

[3] R. Khanna, Q. Zhang, W. E. Stanchina, G. F. Reed, and Z.-H. Mao, "Maximum power point tracking using model reference adaptive control," *IEEE Trans. Power Electron.*, vol. 29, no. 3, pp. 1490–1499, Mar. 2014.

[4] N. Khaehintung, A. Kunakorn, and P. Sirisuk, "A novel fuzzy logic control technique tuned by particle swarm optimization for maximum power point tracking for a photovoltaic system using a current-mode boost converter with bifurcation control," *Int. J. Control, Automat. Syst.*, vol. 8, no. 2, pp. 289–300, Apr. 2010.

[5] I. Batarseh, *Power Electronics Circuits*. Hoboken, NJ, USA: Wiley, 2004.

[6] J. Linares-Flores, A. H. Méndez, C. García-Rodríguez, and H. Sira-Ramírez, "Robust nonlinear adaptive control of a 'boost' converter via algebraic parameter identification," *IEEE Trans. Ind. Electron.*, vol. 61, no. 8, pp. 4105–4114, Aug. 2014.

[7] R. Ortega, A. L. Perez, P. J. Nicklasson, and H. Sira-Ramírez, *Passivity-Based Control of Euler-Lagrange Systems: Mechanical, Electrical and Electromechanical Applications*. London, U.K.: Springer-Verlag, 1998.

[8] Y.-X. Wang, D.-H. Yu, and Y.-B. Kim, "Robust time-delay control for the DC-DC boost converter," *IEEE Trans. Ind. Electron.*, vol. 61, no. 9, pp. 4829–4837, Sep. 2014.

[9] S. Mariethoz *et al.*, "Comparison of hybrid control techniques for buck and boost DC-DC converters," *IEEE Trans. Control Syst. Technol.*, vol. 18, no. 5, pp. 1126–1145, Sep. 2010.

[10] T. Noguchi, S. Togashi, and R. Nakamoto, "Short-current pulse-based maximum-power-point tracking method for multiple photovoltaic-and-converter module system," *IEEE Trans. Ind. Electron.*, vol. 49, no. 1, pp. 217–223, Feb. 2002.

[11] M. H. Todorovic, L. Palma, and P. N. Enjeti, "Design of a wide input range DC–DC converter with a robust power control scheme suitable for fuel cell power conversion," *IEEE Trans. Ind. Electron.*, vol. 55, no. 3, pp. 1247–1255, Mar. 2008.

[12] E. Vidal-Idiarte, L. Martinez-Salamero, J. Calvente, and A. Romero, "An H_∞ control strategy for switching converters in sliding-mode current control," *IEEE Trans. Power Electron.*, vol. 21, no. 2, pp. 553–556, Mar. 2006.

[13] G. E. Pitel and P. T. Krein, "Trajectory paths for DC–DC converters and limits to performance," in *Proc. IEEE Workshops Comput. Power Electron.*, Troy, NY, USA, Jul. 2006, pp. 40–47.

[14] I. H. Kim and Y. I. Son, "Regulation of a DC/DC Boost converter under parametric uncertainty and input voltage variation using nested reduced-order PI observers," *IEEE Trans. Ind. Electron.*, vol. 64, no. 1, pp. 552–562, Jan. 2017.

[15] H. Guldemir, "Sliding mode control of DC-DC boost converter," *J. Appl. Sci.*, vol. 5, no. 3, pp. 588–592, 2005.

[16] J. Fan, S. Li, J. Wang, and Z. Wang, "A GPI based sliding mode control method for boost DC-DC converter," in *Proc. IEEE Int. Conf. Ind. Technol. (ICIT)*, Taipei, Taiwan, Mar. 2016, pp. 1826–1831.

[17] R.-J. Wai and L.-C. Shih, "Design of voltage tracking control for DC–DC boost converter via total sliding-mode technique," *IEEE Trans. Ind. Electron.*, vol. 58, no. 6, pp. 2502–2511, Jun. 2011.

[18] S. Oucheriah and L. Guo, "PWM-based adaptive sliding-mode control for boost DC-DC converters," *IEEE Trans. Ind. Electron.*, vol. 60, no. 8, pp. 3291–3294, Aug. 2013.

[19] S.-K. Kim and K.-B. Lee, "Robust feedback-linearizing output voltage regulator for DC/DC boost converter," *IEEE Trans. Ind. Electron.*, vol. 62, no. 11, pp. 7127–7135, Nov. 2015.

[20] W. He, S. Li, J. Yang, and Z. Wang, "Incremental passivity based control for DC-DC boost converter with circuit parameter perturbations using nonlinear disturbance observer," in *Proc. 42nd Annu. Conf. IEEE Ind. Electron. Soc. (IECON)*, Florence, Italy, Oct. 2016, pp. 1353–1358.

[21] I. H. Kim and Y. I. Son, "Robust cascade control of DC/DC boost converter against input variation and parameter uncertainties," in *Proc. Amer. Control Conf. (ACC)*, Chicago, IL, USA, Jul. 2015, pp. 2567–2572.

[22] H. Sira-Ramírez, A. Hernández-Méndez, J. Linares-Flores, and A. Luviano-Juárez, "Robust flat filtering DSP based control of the boost converter," *Control Theory Technol.*, vol. 14, no. 3, pp. 224–236, Aug. 2016.

[23] R. Silva-Ortigoza, H. Sira-Ramírez, and V. M. Hernández-Guzmán, "Control por modos deslizantes y planitud diferencial de un convertidor de CD/CD boost: Resultados experimentales," *Revista Iberoamer. Automática Inf. Ind.*, vol. 5, no. 4, pp. 77–82, Oct. 2008.

[24] H. Sira-Ramírez and R. Silva-Ortigoza, *Control Design Techniques in Power Electronics Devices*. London, U.K.: Springer, 2006.

[25] H. Sira-Ramírez, R. Ortega, P. Martin, P. Rouchon, and R. Márquez, "Regulation of DC-TO-DC power converters: A differential flatness approach," *IFAC Proc. Volumes*, vol. 29, no. 1, pp. 2442–2447, Jun./Jul. 1996.

[26] R. Silva-Ortigoza *et al.*, "A trajectory tracking control for a boost converter-inverter-DC motor combination," *IEEE Latin Amer. Trans.*, vol. 16, no. 4, pp. 1008–1014, Apr. 2018.

[27] V. H. García-Rodríguez, R. Silva-Ortigoza, E. Hernández-Márquez, J. R. García-Sánchez, and H. Taud, "DC/DC boost converter–inverter as driver for a DC motor: Modeling and experimental verification," *Energies*, vol. 11, no. 8, p. 2044, Aug. 2018.

[28] H. Sira-Ramírez, R. Márquez, F. Rivas-Echeverría, and O. Llanes-Santiago, *Control de Sistemas no Lineales Linealización Aproximada, Extendida y Exacta*. Madrid, Spain: Prentice-Hall, 2005.

[29] S.-D. Lee and S. Jung, "Practical implementation of a factorized all pass filtering technique for non-minimum phase models," *Int. J. Control, Automat. Syst.*, vol. 16, no. 3, pp. 1474–1481, Jun. 2018.

[30] M. Fliess, H. Sira-Ramírez, and R. Márquez, "Regulation of non-minimum phase outputs: A flatness based approach," in *Perspectives in Control*, D. Normand-Cyrot, Ed. London, U.K.: Springer, 1998.

[31] W. Shockley, "The theory of p-n junctions in semiconductors and p-n junction transistors," *Bell Syst. Tech. J.*, vol. 28, no. 3, pp. 435–489, Jul. 1949.

[32] J. Ebers and J. L. Moll, "Large-signal behavior of junction transistors," *Proc. IRE*, vol. 42, no. 12, pp. 1761–1772, 1954.

[33] M. Fliess, J. Lévine, P. Martin, and P. Rouchon, "Flatness and defect of non-linear systems: Introductory theory and examples," *Int. J. Control*, vol. 61, no. 6, pp. 1327–1361, Jan. 1995.

[34] H. Sira-Ramírez and S. K. Agrawal, *Differentially Flat Systems* (Control Engineering Series). Boca Raton, FL, USA: CRC Press, 2004.

[35] R. Silva-Ortigoza, F. Carrizosa-Corral, J. J. Gálvez-Gamboa, M. Marcelino-Aranda, D. Muñoz-Carrillo, and H. Taud, "Assessment of an average controller for a DC/DC converter via either a PWM or a sigma-delta-modulator," *Abstract Appl. Anal.*, vol. 2014, pp. 1–17, Nov. 2014. doi: 10.1155/2014/196010.

[36] G. M. Masters, *Renewable and Efficient Electric Power Systems*. Hoboken, NJ, USA: Wiley, 2004.

LEOPOLDO GIL-ANTONIO received the B.S. degree in electronics and communications from the Technological University of Mexico, in 2003, and the M.S. degree in automatic control from the Center for Technological Innovation and Development in Computing, National Polytechnic Institute, Mexico, in 2010. He is currently pursuing the Ph.D. degree with the Faculty of Engineering, Autonomous University of the State of Mexico. He has been a Research Professor with the Technological Superior Studies of Jocotitlán, since 2010. His research interest includes the theory and application of automatic control in power electronic systems and photovoltaic systems.

BELEM SALDIVAR received the B.S. degree in electronics and telecommunications engineering from the Autonomous University of Hidalgo State, Universidad Autónoma del Estado de Hidalgo, Mexico, in 2007, the M.S. degree in automatic control from the Center for Research and Advanced Studies, National Polytechnic Institute CINVESTAV, Mexico, in 2010, and the Ph.D. degree in automatic control from CINVESTAV and in informatics and its applications from the Research Institute of Communication and Cybernetics of Nantes, IRCCyN, Nantes, France, in 2013. In 2013, she was an Assistant Professor with the Polytechnic University of Pachuca, Hidalgo, Mexico. From 2013 to 2014, she was a Postdoctoral Fellow with the École Supérieure d'Électricité, Supélec, L2S, Gif-Sur-Yvette, France.

Since 2014, she has been a Research Professor of the Cátedras CONACyT Program with the Faculty of Engineering, Autonomous University of the State of Mexico. She has coauthored several articles in recognized journals and international conference proceedings and one book. Her research interests include modeling and control of (finite and infinite-dimensional) dynamic systems, nonlinear and time delay systems, and power electronic systems for photovoltaic applications. Since 2015, she has been a member of the CONACyT National System of Researchers.

OTNIEL PORTILLO-RODRÍGUEZ received the B.S. degree in electronics engineering from Toluca Institute of Technology, Toluca, Mexico, in 2001, the M.S. degree in electronics systems from the Monterrey Institute of Technology and Higher Education, Toluca, Mexico, in 2002, and the Ph.D. degree in perceptual robotics from Scuola Superiore Sant'Anna, Pisa, Italy, in 2008.

From 2002 to 2003, he was a Research Assistant with the Mobile Robotics Laboratory, Monterrey Institute of Technology and Higher Education, Mexico City Campus. From 2004 to 2008, he was a Research Assistant with the Perceptual Robotics Laboratory, Pisa. Since 2011, he has been an Associate Professor of mechatronics systems with the School of Engineering, Autonomous University of the State of Mexico, Toluca, Mexico. His research interest includes design of electronics drivers for DC motors and photovoltaic applications to be used in medical robots.

GERARDO VÁZQUEZ-GUZMÁN received the B.S. degree in electronic engineering from the Technical Institute of Apizaco, Tlaxcala, Mexico, in 2003, the M.S. degree in electronic engineering from the National Center of Research and Technological Development, Cuernavaca, Mexico, in 2006, and the Ph.D. degree in electrical engineering from the Technical University of Catalonia, Barcelona, Spain, in 2013.

In 2009, he was a Visiting Scholar with Aalborg University, Aalborg, Denmark. Since 2012, he has been with the Technological Institute of Superior Studies of Irapuato holding a full time Professor–Researcher position with the Electronics Department. His research interests include the analysis and design of power electronics converters, renewable energy systems, and grid connected converters.

SAÚL MONTES DE OCA-ARMEAGA received the B.S. degree in mechanical engineering and the M.S. degree in automation from the Tecnológico de Monterrey, Mexico, in 2003 and 2006, respectively, and the master's and Ph.D. degrees in automatic, robotics and vision from the Technical University of Catalonia (UPC), Barcelona, Spain, in 2011.

He has published several papers in international conference proceedings. His current research interests include the fault detection and isolation, and fault-tolerant control of dynamic systems. He is a member of the CONACyT National System of Researchers.

• • •